Competition between Local Collisions and Collective Hydrodynamic Feedback Controls Traffic Flows in Microfluidic Networks

M. Belloul,[1] W. Engl,[2] A. Colin,[2] P. Panizza,[1,*] and A. Ajdari[3]
[1]IPR, UMR CNRS 6251, Campus Beaulieu, Université Rennes 1, 35042 Rennes, France
[2]LOF, CNRS-Rodia 5258, Université Bordeaux 1, 33608 Pessac, France
[3]Physico-Chimie Théorique, UMR CNRS Gulliver 7083, 10 rue Vauquelin, 75231 Paris, France
(Received 11 December 2008; published 13 May 2009)

By studying the repartition of monodisperse droplets at a simple T junction, we show that the traffic of discrete fluid systems in microfluidic networks results from two competing mechanisms, whose significance is driven by confinement. Traffic is dominated by collisions occurring at the junction for small droplets and by collective hydrodynamic feedback for large ones. For each mechanism, we present simple models in terms of the pertinent dimensionless parameters of the problem.

DOI: 10.1103/PhysRevLett.102.194502 PACS numbers: 47.61.−k, 47.55.D−

When studying flows of dispersions in microfluidic networks, a central goal is to understand the mechanisms that govern flow partitioning at the nodes. Known as ''plasma skimming'' in blood microcirculation, this issue is fundamental for well functioning cardiovascular systems [1], whereas in digital microfluidic devices it is essential for the traffic flow control of droplets [2]. This problem is also challenging in the field of nonlinear physics. For instance, consider the simplest situation where a droplet train reaches a T intersection and ask how the droplets divide between the two outlets. When a droplet arrives at the junction, it flows into the arm having the lowest hydrodynamic resistance. Since the presence of droplets in microchannels increases the resistance to flow, there is a nonlinear collective feedback between successive droplets' trajectories [3,4]. The outcome turns out to be a complex nonlinear dynamical system, now drawing much interest as it lays the foundations of promising applications for the design of logical microfluidic devices [5–7].

In this Letter, we demonstrate the crucial role played by confinement and dilution on the traffic of discrete fluid elements in microfluidic networks. To address this issue, we study the repartition of trains of monodisperse droplets at a T junction. By systematically varying the asymmetry of the junction, the dilution, and the confinement of the droplets, we show that droplet traffic results from the competition of two distinct physical mechanisms, governed by the confinement. Traffic is dominated by local collisions, occurring at the junction for small droplets, whereas it results from collective hydrodynamic feedback (CHF) for large ones. For each regime, simple models, yielding universal behaviors in terms of the relevant dimensionless numbers of the problem, are proposed and tested in experiments. These models capture the main features of the problem and provide a general picture of traffic flows in microfluidic networks.

Experiments.—In our experiments (inset, Fig. 1), a periodic train of water-oil monodisperse droplets is produced using a double cylindrical capillary module, consisting of a calibrated syringe needle (diameter 510 μm or 230 μm) centered in a tube (radius $r_c = 750$ μm). Using two syringe pumps (Harvard PHD 2000), millipore water (viscosity $\eta_w = 1$ mPa s) and sunflower oil (from Maurel Inc., France, viscosity $\eta_o = 50$ mPa s) are, respectively, infused through and around the central needle, so that droplets form at the tip of the needle with a constant rate of production, f. By fine-tuning both Q_w and Q_o^f, the respective flow rates of water and oil, we control Ω, the droplet volume. An additional infusion of oil performed downstream, at constant flow rate Q_o^d, increases λ, the distance between two successive droplets while keeping their size unchanged. The behavior of this train at a bifurcation is studied by directing it towards a simple asymmetric T junction whose outlets have different lengths, $L_2 > L_1$, but the same cross sections and whose two extremities are connected to the same air pressure P_o. Images of the

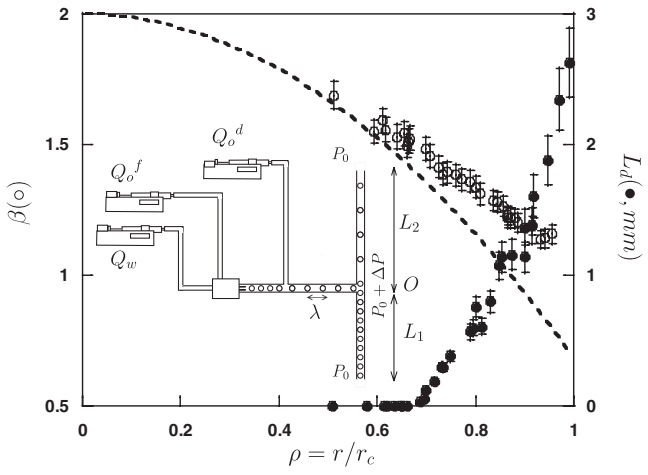

FIG. 1. β (○) and L_d (●), versus ρ. The dashed line corresponds to the asymptotic model of [9]: $\beta = 2 - \frac{4\eta}{3\eta+2}\rho^2$ where $\eta = \frac{\eta_o}{\eta_w}$. Inset: Schematic of the setup.

 © 2009 The American Physical Society

flow at the junction are captured and recorded with a video camera. We limit our studies to droplets having size r smaller than r_c so that they do not deform due to confinement and do not break up at the junction [8]. The capillary and Reynolds numbers at play in our experiments are, respectively, of the order of 10^{-2} and 10^{-1}.

Transport of droplets in a constant section tube.—Understanding droplet flows in microfluidic networks first requires the description of droplet transport in a simple linear channel of constant section S. We prepare a train of monodisperse droplets and systematically increase λ (i.e., the dilution flux), while keeping Ω and f fixed. We measure the constant droplet velocity U and the pressure drop δP for a tube of length L. To characterize the influence of confinement on droplet flow, we systematically vary Ω and discuss our results in terms of $\rho = \frac{r}{r_c}$, a dimensionless number characterizing droplet confinement. In all our experiments, we observe that $U = \beta \frac{Q}{S}$ with $Q = Q_w + Q_o^f + Q_o^d$ and $1 < \beta < 2$, a dimensionless coefficient function of ρ (Fig. 1). For small values of ρ, the variation of β with ρ is well described by the formula analytically derived by Hetsroni, Haber, and Wacholder [9] for an isolated spherical droplet flowing in a cylindrical channel. The droplets in this first experiment are therefore sufficiently distant and small so that they do not interact directly with each other and do not rub against the walls with a friction that depends on the capillary number, as in the Bretherton regime [10]. From the measurement of δP, we compute the hydrodynamic resistance $\Gamma(L, \Omega, \lambda) = \frac{\delta P}{Q}$ of the portion of tube length L, filled with $n = \frac{L}{\lambda}$ droplets of volume Ω. For any value of Ω, we observe that $\Gamma(L, \Omega, \lambda) = \Gamma_o(L)(1 + \frac{L_d}{\lambda})$ where Γ_o and L_d are, respectively, the hydrodynamic resistance of the tube with no droplets and the characteristic excess length added by each droplet to the tube in terms of hydrodynamic resistance. The variations of L_d reported in Fig. 1 reveal the existence of two distinct regimes: L_d strongly increases with ρ above a critical value of confinement, $\rho_c \simeq 0.7$, whereas its value is essentially zero below ρ_c.

Traffic at a T *junction.*—Let us now investigate and demonstrate the direct influence of confinement on flow partitioning at a simple T junction. We have previously shown [3] the existence of a hydrodynamic transition between a first regime where the droplets partition at the junction between the two outlets and another so-called filter regime where they all collect into the shortest one. At low dilution, the droplets divide between the two outlets; for higher dilution, they all collect into the outlet whose length is the shortest. The repartition-filter (R-F) transition occurs for a well defined value of the dilution, $\lambda = \lambda_f$. To elucidate the key role of confinement on the mechanisms of droplet repartition at the junction, we now perform a systematic study of the onset of this transition as a function of $\Lambda = \frac{L_2}{L_1}$, the asymmetry ratio of the junction and ρ. The inset of Fig. 2 displays λ_f versus ρ, for three different values of Λ. For all values of ρ, λ_f is a decreasing function of Λ, indicating that the asymmetry of the junction clearly favors the filter regime over droplet partitioning. The effect of confinement is however more complex to understand, since all curves present two regimes: for $\rho < 0.85$, λ_f is nearly constant, whereas for $\rho > 0.85$ it strongly increases with ρ. In what follows, we will demonstrate that this general feature results from the competition between two physical mechanisms driven by the confinement.

Discussion.—When a droplet arrives at the junction, it follows the dominant stream and flows into the outlet having the largest flow rate. At high dilution, it systematically goes into the shortest arm; this arm has the lowest hydrodynamic resistance since no droplets are present in any outlet. This is the filter regime obtained for $\lambda > \lambda_f$. However, for lower dilution, the droplets which flow into the shortest sidearm may increase its hydrodynamic resistance sufficiently so that it eventually overcomes that of the other arm. If so, the next droplet reaching the junction goes into the emptied longer arm: this is the repartition regime observed for $\lambda < \lambda_f$. Within this picture, the value of λ_f corresponds to the situation where the hydrodynamic resistance of the shortest arm filled with droplets becomes equivalent to that of the longest outlet where no droplets are present. Along these lines, a straightforward calculation predicts that $\lambda_f = \frac{2L_d}{\Lambda - 1}$ [3]. We test the validity of this approach by plotting the master curve $(\Lambda - 1)\lambda_f$ versus ρ and compare it to the experimental values of $2L_d$ (Fig. 2). Excellent agreement is found when $\rho > 0.85$, indicating that for large (i.e., confined) droplets, traffic at the junction does result from CHF due to the presence of droplets in the outlets. However, by contrast for unconfined droplets (i.e., for $\rho < 0.75$), a strong discrepancy is observed between

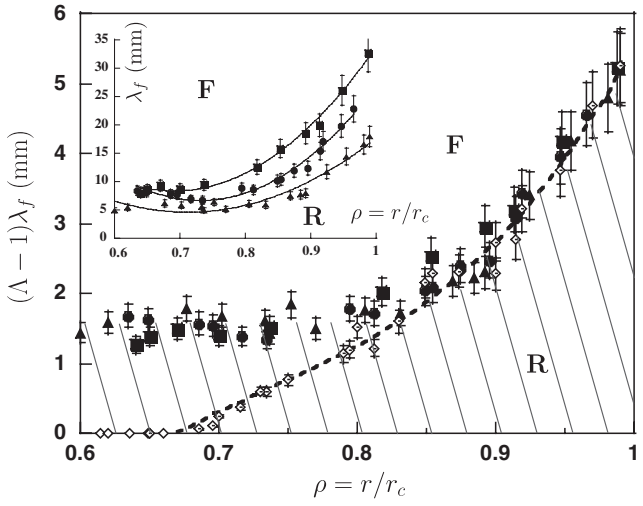

FIG. 2. Plotted are the master curve $\lambda_f(\Lambda - 1)$ [for $\Lambda = 1.14$ (■), $\Lambda = 1.2$ (●), and $\Lambda = 1.34$ (▲)] and $2L_d$ (◇) versus ρ. R (striped area) and F stand, respectively, for the repartition and filter regimes. Inset: λ_f versus ρ.

the prediction of the CHF model and our experimental results. In this ρ region, the droplets cannot contribute to collective hydrodynamic feedback since they do not add significant hydrodynamic resistance to a tube through which they flow (Fig. 1). We thus expect to obtain filtering for all λ values, whereas, surprisingly, we still observe partitioning of the droplets over a large domain of dilution. This raises two fundamental questions. What is the new physical mechanism different from collective hydrodynamic feedback that promotes the presence of droplets in the longest outlet in this ρ region? Why is the role of confinement so important for droplet traffic?

We gain insight into this new and unexpected mechanism by observing the flow of small droplets at the junction. Surprisingly, we witness collisions between successive droplets (Fig. 3).

We notice that a direct consequence of these collisions occurring at the junction is the stabilization of the repartition regime over the filter one (small colliding droplets always distribute in different outlets). To check whether the *R-F* transition in the low ρ region results solely from these collisions, we perform systematic observations of the flow at the junction for different values of ρ and dilutions. We progressively vary the dilution flux measured by λ at fixed drop size and f and measure the probabilities that a collision occurs at the junction (P_c) and that a droplet bifurcates towards the longest outlet (P_2).

Results reported in Fig. 4 show that collisions are observed for values of λ smaller than a critical value λ_c. For $\rho < 0.75$, we note that $\lambda_c \simeq \lambda_f$, a proof that partitioning in this ρ region results from collisions. By contrast, for $\rho > 0.8$, collisions are only observed far from the *R-F* transition ($\lambda_c \ll \lambda_f$), a region not investigated in our previous work [3].

To understand the promotion of collisions at a T junction, let us consider in the filter regime a droplet (k) of radius r_k reaching the stagnation point O of the junction where the pressure is $P_o + \Delta P$. It is submitted to a net force, due to the pressure difference exerted on its two hemispheres by the flows of the two outlets. This force can be roughly approximated by $F = \alpha[p_1(r_k) - p_2(r_k)]r_k^2$, with α and $p_i(r_k)$ being, respectively, a numerical coefficient and the pressure in outlet i at distance r_k from O. In the unconfined region, the pressure profiles in each outlet are linear but have different slopes, related to the values of the total flow rates in each arm. Within this picture, a direct calculation leads to

$$F = \alpha r_k^3 \frac{8\eta_o}{\pi r_c^4} \frac{\Lambda - 1}{\Lambda + 1} Q. \quad (1)$$

Under the action of this force, the droplet moves laterally to the shortest sidearm with a velocity V_{junc}, which at low capillary and Reynolds numbers (and neglecting droplet inertia) varies as $V_{\text{junc}} = \mu(r_k)F$. $\mu(r_k)$ is a mobility coefficient which depends on the droplet size r_k. Its value can be estimated by noting that in the limit $\Lambda \to \infty$, $V_{\text{junc}} = \beta(\rho_k)\frac{Q}{S}$. When the $(k+1)$ drop reaches O, a time τ_k has elapsed. The condition for a collision to occur between these two droplets is given by $\tau_k \lesssim t_k$, where the retention time of droplet (k) at the junction, t_k, is roughly $t_k \simeq r_k/V_{\text{junc}}$, and τ_k is the time span between the productions of the two droplets (k) and $(k+1)$. The inset of Fig. 4 displays the distributions of times τ_k and t_k, measured for $\rho = 0.6$ and $\Lambda = 1.14$. We note that (i) the distribution of

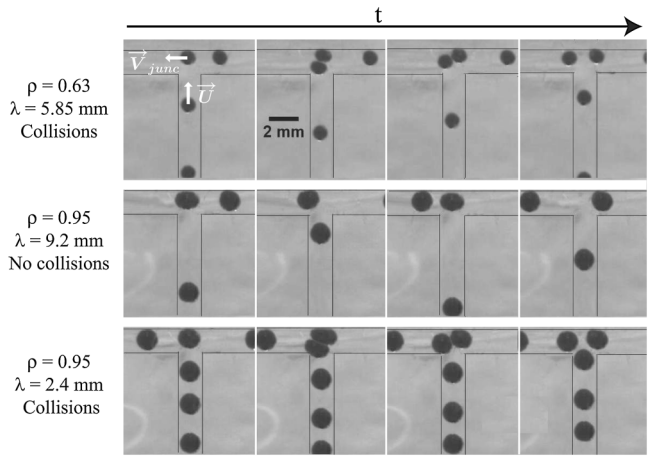

FIG. 3. Snapshots of successive droplets reaching the junction in different hydrodynamic regimes. Top line: Repartition of small droplets with collisions ($\Lambda = 1.14$) [see movie1.avi in the supplementary material, (a) in [11]]. Center and bottom lines: Repartition of large droplets in the CHF regime with no collisions (center line) and in the collision regime (bottom line) ($\Lambda = 1.34$) [see movie2.avi, (a) in [11], and movie3.avi, (c) in [11]].

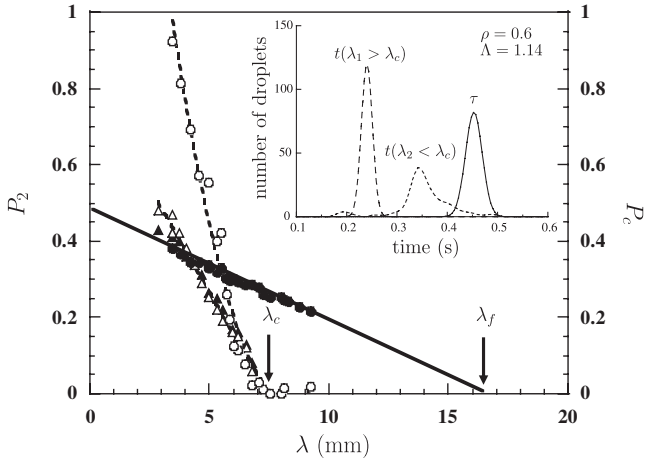

FIG. 4. Shown are (P_2) (closed symbols) and (P_c) (open symbols) versus ρ for $\rho = 0.99$ (circles) and $\rho = 0.75$ (triangles) and $\Lambda = 1.34$. The equation of the continuous line corresponds to the expression of $P_2 = \frac{1}{\Lambda+1}\left[1 - \frac{(\Lambda-1)\lambda}{2L_d}\right]$, predicted by the CHF theory [12]. The dashed lines are guide for the eyes. Inset: Distributions of the production time, τ, and the retention times, t, measured over 200 droplets for $\lambda_1 = 11.5$ mm and $\lambda_2 = 7$ mm.

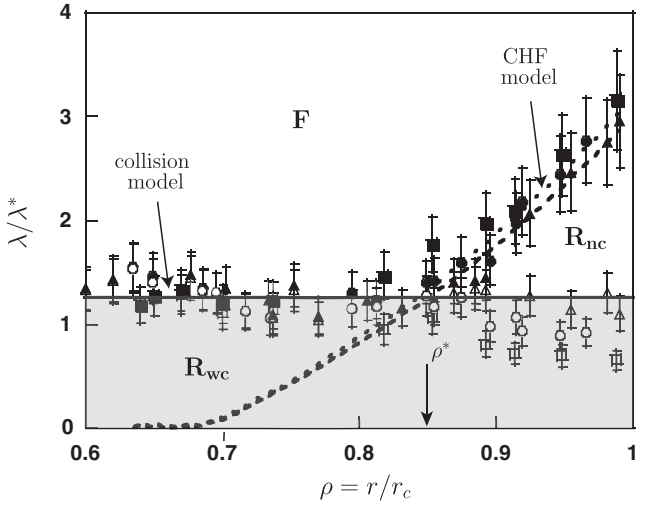

FIG. 5. Shown are $\frac{\lambda_c}{\lambda^*}$ (open symbols) and $\frac{\lambda_f}{\lambda^*}$ (filled symbols) plotted as a function of ρ. $\Lambda = 1.14$ (squares), $\Lambda = 1.2$ (circles), and $\Lambda = 1.34$ (triangles). The dashed line is the best horizontal fit of the data for small values of ρ. The short- and long-dashed lines correspond, respectively, to the quantity $\frac{2L_d}{(\Lambda+1)\rho r_c}$ computed for $\Lambda = 1.2$ and $\Lambda = 1.34$. F, R_{nc}, and R_{wc} stand, respectively, for the filter regime and the repartition regimes without and with collisions. The grey area corresponds to the collision region.

times τ_k peaks around its mean value $\tau = \frac{1}{f}$ (our trains of droplets are almost periodical), (ii) the distributions of the retention times, t_k, are narrow in the filter regime, whereas they become much broader when collisions occur, and (iii) the mean value t of the distribution t_k decreases by diluting the system (i.e., increasing λ). Establishing a complete description of the probability for collisions is a great challenge since (1) the expression of the retention time at the junction depends on the details of the collisions between droplets and (2) the probability that two consecutive droplets collide is very sensitive to fluctuations in τ_k and r_k. However, in a first approximation, to derive an analytical expression for the onset of the collision–no-collision transition we can neglect fluctuations in t_k and in τ_k [because of our observations (i) and (ii)]. By using this mean field approach (i.e., replacing τ_k with τ and r_k with r), the retention time of droplet at the junction is given in the filter regime by $t \simeq \tau \frac{\Lambda+1}{\Lambda-1} \frac{r}{\lambda}$ [a result consistent with our experimental observation (iii)]. The criterion for collisions to occur ($t > \tau$) yields

$$\lambda < \lambda^* \simeq \frac{\Lambda + 1}{\Lambda - 1} \rho r_c \tag{2}$$

We validate this approach that neglects inertia effect (the Weber numbers at play in our experiments are typically of the order 10^{-2}) by plotting $\frac{\lambda_c}{\lambda^*}$ as a function of ρ (Fig. 5). For small values of ρ, good agreement is found: both the experimental Λ and ρ dependence of λ_c coincide with the predictions of the model for λ^* within experimental errors. Furthermore, the value found for $\frac{\lambda_c}{\lambda^*}$ is very close to 1. Despite its simplicity, our model captures the main features of our experimental observations of the R-F transition made for small droplets, whereas for large droplets, the data are well supported by the CHF model. By extrapolating these two models to intermediate values of ρ, an estimate for the crossover between both regimes can be established, namely, $\rho^* \simeq \frac{2L_d}{r_c(\Lambda+1)}$ (see Fig. 5).

To conclude, confinement plays a key role in the traffic flow of the discrete elements of fluids in microfluidic networks. Traffic at a bifurcation is regulated by two distinct mechanisms: local collisions or collective hydrodynamic feedback, whose significance is controlled by the droplet confinement. For each mechanism, models are proposed in terms of the various dimensionless parameters of the problem. Our models provide a general framework for traffic flows in branched geometries. Our results elicit new opportunities for the design of digital microfluidic circuits since the local topology and geometry of a junction (neck or feature hindering droplet motion) are susceptible to modifying the occurrence of collisions at the junction. The conclusions drawn here should be relevant to other systems such as blood microcirculation, respiration, or more general traffic flows.

This work was financed by an ACOMB grant (ref: Droplets) from Brittany (France). We thank L. Courbin and D. A. Sessoms for fruitful discussions.

*pascal.panizza@univ-rennes1.fr

[1] A. S. Popel and P. C. Johnson, Annu. Rev. Fluid Mech. **37**, 43 (2005).
[2] M. Joanicot and A. Ajdari, Science **309**, 887 (2005).
[3] W. Engl, M. Roche, A. Colin, P. Panizza, and A. Ajdari, Phys. Rev. Lett. **95**, 208304 (2005).
[4] F. Jousse, R. Farr, D. R. Link, M. J. Fuerstman, and P. Garstecki, Phys. Rev. E **74**, 036311 (2006).
[5] P. Garstecki, M. J. Fuerstman, and G. M. Whitesides, Nature Phys. **1**, 168 (2005).
[6] M. Prakash and N. Gershenfeld, Science **315**, 832 (2007).
[7] M. J. Fuerstman, P. Garstecki, and G. M. Whitesides, Science **315**, 828 (2007).
[8] D. R. Link, S. L. Anna, D. A. Weitz, and H. A. Stone, Phys. Rev. Lett. **92**, 054503 (2004).
[9] G. Hetsroni, S. Haber, and E. Wacholder, J. Fluid Mech. **41**, 689 (1970).
[10] F. P. Bretherton, J. Fluid Mech. **10**, 166 (1961).
[11] See EPAPS Document No. E-PRLTAO-102-031922 for (a) movie1.avi showing the partitioning of small droplets ($\rho = 0.63$) in the collision regime, (b) movie2.avi showing the partitioning of large droplets ($\rho = 0.95$) in the absence of collisions (CHF regime), and (c) movie3.avi showing the partitioning of large droplets ($\rho = 0.95$) in the collision regime. For more information on EPAPS, see http://www.aip.org/pubservs/epaps.html.
[12] D. A. Sessoms, M. Belloul, M. Roche, W. Engl, L. Courbin, and P. Panizza (to be published).